Suspension-Firing of Biomass

Part 1, Full-Scale Measurements of Ash Deposit Build-up

Bashir, Muhammad Shafique; Jensen, Peter Arendt; Frandsen, Flemming; Wedel, Stig; Dam-Johansen, Kim; Wadenback, Johan; Pedersen, Søren Thaaning

Published in:
Energy & Fuels

Link to article, DOI:
10.1021/ef201680k

Publication date:
2012

Document Version
Publisher's PDF, also known as Version of record

energy&fuels

Article

pubs.acs.org/EF

Suspension-Firing of Biomass. Part 1: Full-Scale Measurements of Ash Deposit Build-up

Muhammad Shafique Bashir,[†] Peter Arendt Jensen,*[,†] Flemming Frandsen,[†] Stig Wedel,[†] Kim Dam-Johansen,[†] Johan Wadenbäck,[‡] and Søren Thaaning Pedersen[‡]

[†]DTU Chemical and Biochemical Engineering, Technical University of Denmark, Building 229, DK-2800 Lyngby, Denmark

[‡]Vattenfall A/S, Amager Power Plant, Kraftværksvej 37, DK-2300 Copenhagen S, Denmark

ABSTRACT: This paper is Part 1 in a series of two describing probe measurements of deposit build-up and removal (shedding) in a 350 MW_{th} suspension boiler, firing straw and wood. The influence of fuel type (straw share in wood), probe exposure time, probe surface temperature (500, 550, and 600 °C), and flue gas temperature (600−1050 °C) on ash deposit formation rate has been investigated. Investigations of deposit formation rate were made by use of an advanced online deposit probe that allowed nearly continuous measurement of the deposited mass. Two different measures of deposit formation rate are used in the analysis of the data. The first is the integral deposit formation rate (IDF-rate) found by dividing the integral mass change over integral time intervals (of order several hours) by the time interval. The IDF-rate is similar to deposit formation rates based on total deposit mass uptake divided by probe exposure time reported in previous full-scale investigations, but it is a relatively crude measure that includes all deposit shedding in addition to actual deposit formation. To remove major shedding events from the determination of deposition rates a second measure, the derivative-based deposit formation rate (DDF-rate), was devised. This was determined by averaging the deposit mass uptake signals over short time intervals (on the order of minutes), calculating the local values of the time derivative of the mass uptake, removing large negative values signifying major shedding events, and finally time smoothing the derivatives to remove excessive noise. The DDF-rate was influenced by flue gas temperature and straw share, while changes in probe surface temperature had no significant influence. The IDF-rate, qualitatively related to the ratio between the time-integrated DDF-rate and the integration time, followed the same trends. Ash transformation was investigated by bulk ash analysis of the fuel, fly, and bottom ash during straw and/or wood suspension firing. Bulk ash analysis of fly ashes showed that the contents of volatile elements (K, Cl, S) were slightly greater than in the fuel ash, while Ca and Si remained either in the same proportion or were slightly reduced. It was also found that, with an increase in fuel ash K/Si molar ratio, the concentration of the volatile elements, K, Cl, and, to some extent, S, increased in the fly ash. The bottom ash was dominated by Si and Ca, with almost no S and Cl, possibly as a result of the high volatility of S and Cl during combustion at higher temperatures.

1. INTRODUCTION

By the end of 2009, there were eight biomass and five biomass cofired power plants in Denmark.[1] Utilization of biomass in power plants is an attractive option to lower CO_2 emissions and to make the energy supply independent of fossil fuels. However, the use of biomass, especially straw, constitutes a serious technical challenge as a result of the presence of large amounts of alkali metals and chlorine.[2−8] The presence of alkali metals and chlorine may induce large operational problems due to boiler ash deposition and subsequent corrosion.[6,8−11] To minimize deposition problems, different strategies can be employed, for example, use of additives that can convert the vaporized inorganic species to less harmful forms, pretreatment of fuels by leaching out alkali, cofiring with coal, and use of effective deposit shedding techniques.[4−8,10,12−18]

Some full-scale experimental studies on ash deposit build-up and removal conducted in biomass grate-fired boilers can be found in the literature.[16−19] Potentially, most suspension-fired boilers have a better electrical efficiency (46−48%) than traditional grate-fired systems (25−30%),[8] but only limited ash deposition data from biomass suspension firing are availabe.[10,14,15,20−25] In biomass suspension firing, pulverized biomass typically from pellets crushed in the coal mills (roller mills) is blown into the burners, where the fuel particles are burned in suspension. Quantification of deposit formation rates in biomass suspension-fired boilers is an area where relatively limited accurate knowledge is available, and improved knowledge on the transient deposit formation and removal is wanted to optimize design and operation.[14,20−22,24] Compared to grate-fired units, the deposit flux may increase during suspension firing because a larger part of the fuel ash is transformed to fly ash.[2] In addition, fuel particle residence times are on the order of a few seconds, and peak flame temperatures are higher, compared to grate firing conditions.[23] Investigations by Nordgren et al.[20] indicate that, during biomass (straw and/or woody biomass) dust combustion at higher temperatures, significant ash deposition formation may appear. Investigations of biomass suspension combustion at both pilot-scale and full-scale have shown higher deposit formation rate during straw firing, compared to straw and wood cofiring, possibly due to dilution and/or chemical interations.[20,24,25] However, only few full-scale measurements are reported for 100% straw and/or wood combustion in suspension-fired boilers, and most of these studies have been based on short testing time (up to 12 h),[14,22] while more

Received: October 28, 2011
Revised: February 21, 2012
Published: March 20, 2012

extensive full-scale measurements are rare.[24] Therefore, detailed and extensive full-scale studies on transient deposit formation processes when firing straw and wood will improve our understanding of ash deposit formation processes.

The aim of this study is to provide long-time, full-scale data on ash deposit formation in a 350 MW_{th} suspension-fired boiler, firing straw and wood. Furthermore, an analysis is carried out, giving quantitative information about deposit formation rates as functions of operating conditions. The influence of fuel type (straw share in wood), probe exposure time, probe surface temperature (500, 550, and 600 °C) and flue gas temperature (600−1050 °C) on ash deposit formation rate has been investigated.

2. EXPERIMENTAL SECTION

2.1. Boiler. The probe measurements were conducted at Amager Power Station, Unit 1 (AMV1), firing biomass in suspension. The AMV1 boiler, a multifuel suspension-fired boiler, was commissioned in 2009 to use pulverized biomass with varying shares of straw and wood. The annual biomass consumption (AMV1) is approximately 300 000 tons wood pellets and 100 000 tons straw pellets. The 350 MW_{th} boiler is front wall-fired with 12 burners at 3 levels. The fuel is introduced as particles and is combusted while being suspended in the air stream. Due to an expected increase in the corrosion rate with respect to temperature, the final steam temperatures of the superheaters are limited to approximately 540 °C.[26] The overall boiler operational data can be found in Table 1, while the boiler drawings with identified probe measuring position are shown in Figure 1. Only one probe position was selected. The probe measuring position was selected because of significant deposit build-up during straw firing in that boiler position. The selected probe measuring position was in the most contaminated area in the boiler.

Table 1. Brief Operational Data of the AMV1 Boiler

param. (steam)	unit	high pressure (HP) superheater	reheater (RH)
temp.	°C	540 (biomass)	540
pressure	bar	185	75
flow	kg/s	138.4	123

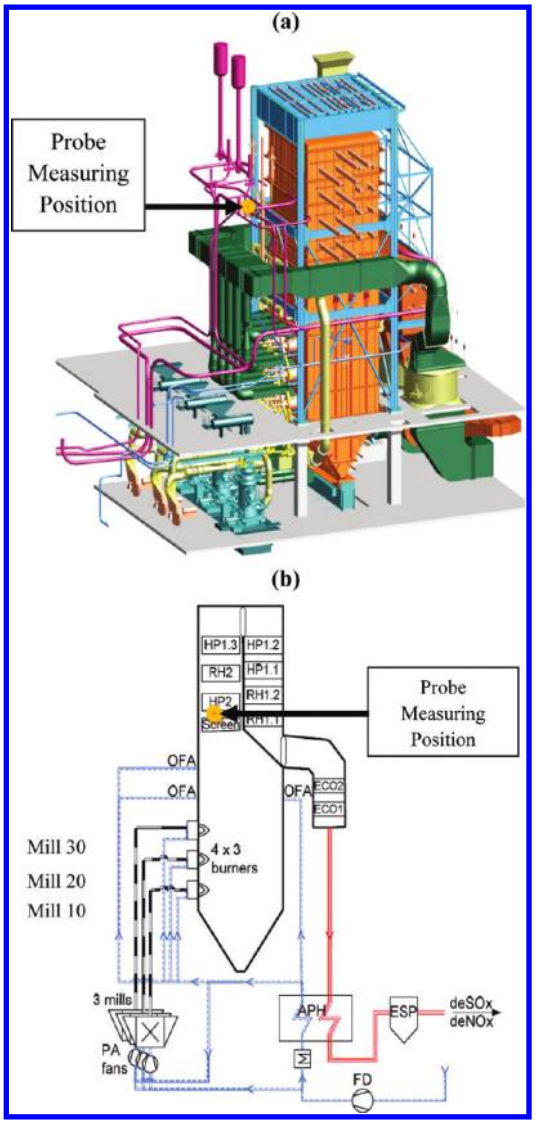

Figure 1. Drawings of AMV1 boiler with identified probe measuring position, just above the screen tubes: (a) overall boiler configuration, (b) schematic presentation of the boiler. (Modified with permission from ref 26. Copyright 2006, Power-Gen Europe.) Top: mill 30. Middle: mill 20. Bottom: mill 10. HP: high pressure. RH: reheater. OFA: over fire air. ECO: economizer. APH: air preheater.

2.2. Ash Deposition Probe. The deposit probe used during the measurements is shown schematically in Figure 2a and b. The probe is made of stainless steel, is about 3 m long, and has an outer diameter of 40.5 mm. The probe was cooled by water and air, whereby it was possible to determine heat uptake by the probe and keep a stable surface temperature. The probe hung on a hinge connected to a flange. A balance at the rear was used to oppose fluctuations in the boiler and to keep the probe aligned horizontally. A load cell was used to detect the force caused by the mass of deposit on the probe. The deposit mass was calculated by using the following balance:

$$m_{dg} = (m_{t0} - m_{t1})g\frac{L_1}{L_2} \quad (1)$$

where m_d is the deposit mass (g), g is the gravitational acceleration (m/s^2), m_{t0} is the initial mass signal of the load cell (g), m_{t1} is the final mass signal of the load cell (g), and L_1 and L_2 are the distances (mm) from the hinge to the balance (784 mm) and to the mass center of the deposit (1460 mm), respectively. The deposit mass signals were then divided by the probe surface area to get a measure of the deposit mass uptake.

In each horizontal position of the probe (TC position 1, 2, and 3), four thermocouples provided temperatures at the N, E, S, and W positions (Figure 2b). A CCD (charge-coupled device) camera registered the deposit formation and removal processes on the probe. The flue gas temperature near the probe was continuously measured, using a simple thermocouple in a protective shell. In addition, a suction pyrometer (International Flame Research Foundation (IFRF) model[27]) was also used for some periods during each test. Due to strong radiation effects in the probe measuring area, a significant difference was identified between the flue gas temperature measured by the thermocouple and the suction pyrometer. A schematic of the port used during the measurements is shown in Figure 2c. In the large port, a small port for the deposit probe, a port for the thermo-element, a CCD camera port, and a port for the suction pyrometer and artificial sootblowing probe can be seen. The thermocouple was placed just above the suction pyrometer port.

2.3. Fuels. The compositions and analysis methods of some of the fuels fired during the full-scale measurements are shown in Table 2. It is seen that the straw ash has a high content of Si, K, and Ca. During the experiments, the fuels were continuously sampled before the burners and then analyzed. The ash contents of the fuel from all test runs were analyzed, and thereby, the straw fuel fractions were determined based on the total ash contents. The detailed ash analysis was done on samples from test 1 and test 5, as shown in Table 2.

Overall, eight test runs were carried out, and the mean straw share during each test is shown in Table 3. In Table 3, mean values of each complete test are shown, while in Table 2 values are shown for a

dx.doi.org/10.1021/ef201680k | Energy Fuels 2012, 26, 2317−2330

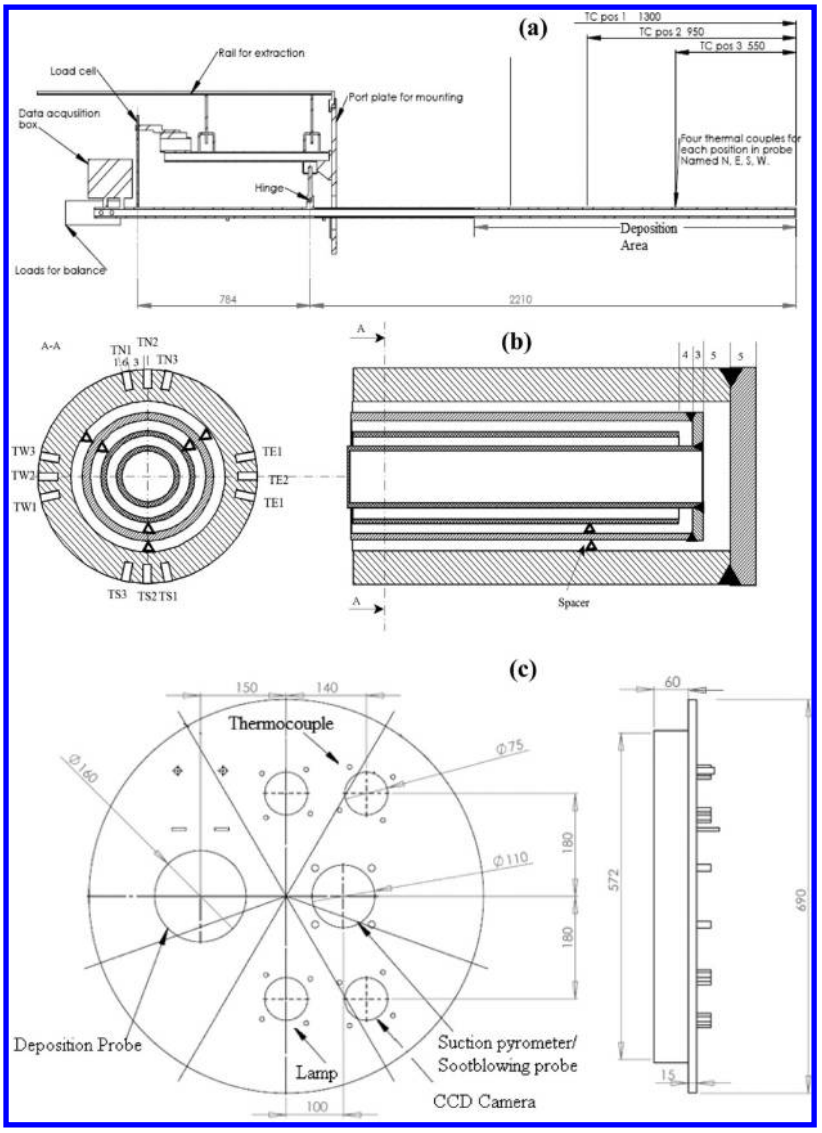

Figure 2. Schematic presentation of the probe and the complete port: (a) schematic view of the probe with identified positions of temperature measurements, deposition area, port plate for mounting, hinge, load cell, and rail for pulling out the probe, (b) cross-sectional view perpendicular to probe axis and cross-sectional view along axis of annuli, (c) schematic drawings of the port plate used during the measurements.

sample collected just before the burners. This causes a slight difference in fuel ash contents reported in Tables 2 and 3. It should be mentioned that the pure straw and wood fuel samples shown in Table 2 were collected from the fuel silos, while fuel sample just before the burners was collected almost daily during each test.

The particle size distribution of the fuel particles collected just before the burners showed that close to 50% of the particles were below 500 μm (Figure 3), while about 10 wt % of the particles had a size between 1.2 and 3.1 mm.

2.4. Procedure of Experiments. A series of probe measurements were conducted in the superheater region, just above the screen tubes. The influence of fuel type, probe exposure time, flue gas temperature and probe surface temperature on deposit formation rate was investigated. The fuel contained from 0 to 85 wt % straw share in wood. Each measurement lasted 2−18 days. The deposition probe was exposed to flue gas temperatures from 600 to 1050 °C. Probe surface temperatures were varied between 500 and 600 °C in order to investigate ash deposit formation rate at different probe surface temperatures. A complete summary of all the conducted measurements is presented in Table 3.

Retractable steam soot blowers were used for 5−10 min (each soot blower) at regular intervals during boiler operation, typically at 8 h intervals. The soot blower located nearest to the probe measuring position (approximately 1 m to the left) was shut down during tests 1−5, while soot blowers located further away from the measuring position were in operation during all the tests.

Ash transformation was investigated by elemental analysis of inorganic elements in the fuel ash, residual ash and deposit samples for different straw shares in wood by ICP-IC (inductively coupled plasma-ion chromatography) analysis. Fly ash was collected from electrostatic precipitators by using a spear to collect a representative sample. Bottom ash was collected from the water and ash pit at the bottom of the furnace.

3. RESULTS AND DISCUSSION

3.1. Data Treatment. The results represented in this paper are from full-scale measurements on a large operating power plant boiler. Hence, full control over all conditions influencing measurements cannot be achieved. In particular, two aspects of the measurements will be considered.

One aspect is the influence of operating conditions on temperature measurements, where the primary data were thermocouple readings of the flue gas temperature. Radiation, flow fluctuations, and particulates in the gas phase can all influence

dx.doi.org/10.1021/ef201680k | Energy Fuels 2012, 26, 2317−2330

Table 2. Analysis of Straw and Wood Pellets Used at AMV1[a]

param.	procedure	straw (Køge)	wood (Kunda*)	80−85% straw (test 1)	65−70% straw (test 5)	60−65% straw (test 5)	60−65% straw (test 5)	40−45% straw (test 5)
day/month/year (time)				22/03/2010	19/04/2010	20/04/2010 (13:00)	20/04/2010 (17:00)	21/04/2010
ash contents (wt %, a.r.)	EN 14775:2009	6.03	0.80	5.26	4.32	3.56	3.63	2.74
ash contents (wt %, d.b.)	EN 14775:2009	6.54	0.86	5.63	4.57	3.78	3.84	2.88
moisture (wt %, a.r.)	EN 14774-3:2009	7.86	6.83	6.67	5.61	5.94	5.55	5.03
higher heating value (MJ/kg, d.b.)	EN 14918:2010	18.71	20.47	17.62	19.68	19.39	19.35	19.87
volatiles (wt %, d.b.)	EN 15148:2009	80.91	85.24	82.87	82.58	82.15		83.11
C (wt %, d.b.)	CEN/TS 15104:2006	50.52	55.54	51.16	52.44	52.89	52.57	53.91
S (wt %, d.b.)	CEN/TS 15289:2006	0.15	0.035	0.121	0.105	0.095	0.093	0.068
N (wt %, d.b.)	DS/EN ISO 10304-1:2009	0.59	0.73	0.8	0.62	0.63	0.68	0.75
H (wt %, d.b.)	EN 14918:2010 calcd.	5.79	6.15	5.85	5.92	5.97	5.96	6.02
O (wt %, d.b.)	EN 14918:2010 calcd.	36.11	36.68	36.43	36.19	36.45	36.67	36.28
Cl (wt %, d.b.)	DS/EN ISO 10304-1:2009	0.290	0.003		0.155	0.184	0.191	0.093
				Ash Analysis (wt %, d.b.)				
Al_2O_3	DIN 51729/ ASTM3682	0.66		0.95	1.88	1.30	0.97	2.11
CaO	DIN 51729/ ASTM3682	14.56		8.30	9.97	11.05	11.80	17.69
Fe_2O_3	DIN 51729/ ASTM3682	0.50		0.47	6.81	1.03	0.58	1.13
K_2O	DIN 51729/ ASTM3682	17.88		15.25	12.58	15.92	20.41	13.96
MgO	DIN 51729/ ASTM3682	3.39		2.25	2.11	2.29	2.54	2.90
Na_2O	DIN 51729/ ASTM3682	0.69		0.57	0.59	0.87	1.04	1.03
P_2O_5	DIN 51729/ ASTM3682	5.56		2.47	2.17	2.46	2.60	2.13
SO_3	DIN 51729/ ASTM3682	2.43		2.36	2.03	2.16	1.88	2.43
SiO_2	DIN 51729/ ASTM3682	44.51		52.05	44.89	49.15	46.95	36.87
TiO_2	DIN 51729/ ASTM3682	0.05		0.06	0.11	0.10	0.06	0.13

[a]a.r.: as received, d.b.: dry basis. * one type out of four.

the readings, but in rather unpredictable ways. Hence, some suction pyrometer readings were taken, and together with determinations of other operating conditions, these measurements allowed a correction of the thermocouple values. The procedure is discussed in detail in section 3.1.1.

The other aspect is the deposit formation rate determinations. In an ideal world, where deposited mass is monitored continuously with little or only insubstantial noise and no deposit shedding, there is no doubt that the time derivative of the mass uptake signal is the true deposit formation rate. However, the measuring probe mass uptake signal, on which this paper is based, includes noise, larger shedding events, and eventually some smaller (minor) shedding events, with a magnitude on the same level as the noise. The shedding events may therefore be divided into two classes: one type of events, macro-events, with so much shedding that the event times mark points across which deposit formation rate calculations cannot be done by averaging, and another type, microevents, that are not clearly distinguishable from externally generated noise contributions, across which it is necessary to do averaging when calculating something that is representative of the true deposit formation rate.

With this kind of measured data, it is necessary to use a terminology that clearly distinguishes between (a) (true) deposition rate, (b) a measure of the deposition rate found as an average of the time derivative over periods that do not include major shedding events but do include some minor shedding events in addition to noise (called derivative-based deposit formation rate, DDF-rate), and finally (c) the overall measure where the difference in deposit mass at two different times is divided by the time difference and, in this case, with no particular concern about the presence or absence of even major shedding events (called integral deposit formation rate, IDF-rate). Each of these measures of deposition rate has its use, but it is important in the discussion of the data to distinguish between them.

The DDF-rate is determined by calculating a smoothed time derivative of the short time averaged deposit mass uptake signals. The time interval for smoothing includes minor shedding events that cannot *a priori* be distinguished from measurement noise but excludes larger shedding events. A more detailed description of the

dx.doi.org/10.1021/ef201680k | Energy Fuels 2012, 26, 2317−2330

Table 3. Experimental Summary of Conducted Measurements

test no.	1	2	3	4	5	6	7	8
day/month/year	22/03/2010 −25/03/2010	27/03/2010 −29/03/2010	29/03/2010 −06/04/2010	06/04/2010 −09/04/2010	15/04/2010 −22/04/2010	07/05/2010 −25/05/2010	25/05/2010 −08/06/2010	08/06/2010 −18/06/2010
straw (wt %)	80−85	60−65	30−35	40−50	40−50	0−10	0−10	0−10
fuel ash content (wt %)	∼5.2	∼4.0	∼2.4	∼3.4	∼3.4	∼1.0	∼1.0	∼1.0
probe temp. (°C)	500	600	500	500	500 (600)	550	550	550 (600)
exposure time (h)	56	45	185	73	168	434	335	212

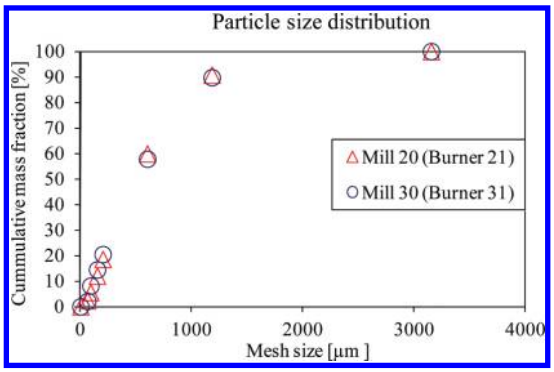

Figure 3. Particle size distribution of fuel collected from two burners connected to two different mills (test 1, 22/03/2011). The particle size distribution was determined by a sieve analysis.

procedure is given in section 3.1.2. Since the averaging time is relatively short, and since a time smoothed derivative is the result, we settled on this measure to be called DDF-rate: derivative-based deposit formation rate. DDF-rates should represent fairly characteristic net-deposition rates, allowing its dependence on operating conditions to be determined.

The IDF-rate is a cruder measure of deposit formation rate determined as the mass deposited on the probe over large time intervals divided by the time interval length. The IDF-rate includes both minor and major shedding events of any kind and is similar to deposit formation rates determined from previous full-scale probe measurement data.[14,24] More details about the procedure are given in section 3.1.3.

3.1.1. Corrected Flue Gas Temperature. The flue gas temperature near the probe was continuously measured, using a simple thermocouple in a protective shell, while suction pyrometer based temperature measurements were only conducted for a limited time during each experiment. The suction pyrometer measurements were conducted for 0.5 to 2 h, ranging from 1 to 3 measurements during each test. During suspension firing of biomass, the radiation effects were stronger compared to biomass grate firing,[17,18] and a typical higher flue gas temperature in the range 50−200 °C was observed by the suction pyrometer. The presence of deposits in the experimental region may cause a difference between thermocouple and suction pyrometer measurements due to changed radiation conditions. Other possible factors responsible for a temperature difference can be the fuel flow through mills located in the top positions (mill 30, top; mill 20, middle; Figure 1) leading to a change in flame position, fuel oil loading, and overall boiler load. These physical causes provided the basis for the initiation of the following empirical model relating a prediction of the gas temperature, Y_{calc}, to the actual measured thermocouple temperature, Y_{TC}:

$$Y_{calc} = Y_{TC} + \mathrm{Diff}_{pred} \quad (2)$$

$$\mathrm{Diff}_{pred} = A + BX_{ash} + CX_{oilload} + DX_{boilerload} + EX_{mill20} + FX_{mill30} \quad (3)$$

X_i in eq 3 represent measured operational parameters likely to influence the difference between the suction pyrometer temperature (Y_{meas}) and the thermocouple temperature (Y_{TC}). X_{ash} (0.70−5.26, wt %) represents the fuel ash content, $X_{oilload}$ (0.0−160.7, MW_{th}) is the fuel oil loading, $X_{boilerload}$ (59.0−93.4, %) is the relative boiler load, and X_{mill} (0.0−7.2, kg/s) denotes the fuel flow rate through the mill indicated. Parameters A−F are empirical constants determined through fitting of the above equations to the true temperatures, Y_{meas}, measured by the suction pyrometer. The fitting was carried out by minimizing the sum of squares (SS). Not all of these operational parameters may have a significant influence on the correction. Hence, we used the methods outlined by Kittrell[28] and Pritchard et al.,[29] based on the variance−covariance matrix, to assess which parameters were most important. The final result of the fitting procedure was that the predicted temperature difference could be described well by eq 4.

$$\mathrm{Diff}_{pred} = BX_{ash} + CX_{oilload} + DX_{boilerload} + EX_{mill20} \quad (4)$$

with the parameters shown in Table 4. The plot of predicted flue gas temperature versus the measured suction pyrometer temperature is shown in Figure 4. It can be seen that the predicted temperature values are close to the measured temperature values.

Table 4. Calculated Constants for Flue Gas Temperature Prediction Model with Estimated Confidence Intervals

constant	value
B	23.11 ± 1.25
C	0.195 ± 0.041
D	0.084 ± 0.068
E	4.78 ± 0.48

dx.doi.org/10.1021/ef201680k | Energy Fuels 2012, 26, 2317−2330

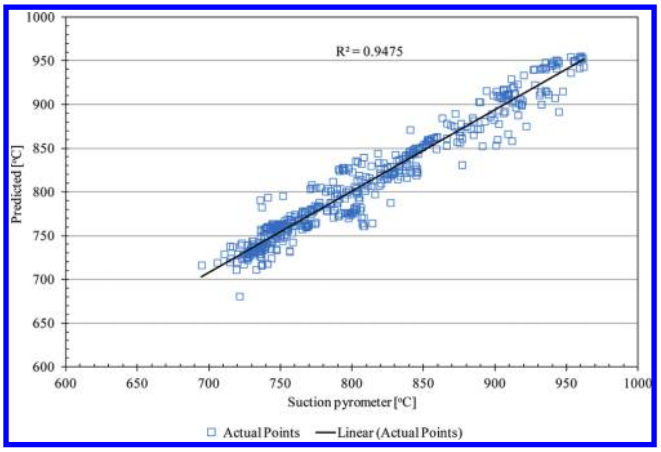

Figure 4. Comparison of measured (suction pyrometer) and calculated flue gas temperature. The predicted points are calculated from the thermo-element temperature and boiler operational data using eqs 2, 3, and 4.

3.1.2. Derivative-Based Deposit Formation Rate (DDF-Rate). The amount of deposit collected on the probe is a function of both the deposit formation process and shedding events. An example of raw data of flue gas temperature, deposit mass uptake, and heat uptake of test 1 is shown in Figure 5. The flue gas temperatures measured using a thermocouple are between 500 and 800 °C. The deposit mass uptake signals show both natural and plant sootblowing shedding events (observed as a sudden deposit mass loss on the curve). The deposit is influenced by several processes: large shedding events, minor shedding events, a relatively slow deposit build-up process, and some noise mainly caused by boiler fluctuations. Boiler fluctuations could be mechanical vibrations or large changes in boiler flow dynamics. The most severe fluctuations are observed when the boiler plant soot blowers were in operation. Even though the plant soot blower nearest to the probe was shutdown, the thermal and mechanical fluctuations were induced by the rest of the soot blowers and that could cause some shedding. To analyze data systematically under these conditions where noise and small and large shedding events are present, a deposit mass uptake signal treatment method is developed and applied to the measuring data. The method allows us to identify shedding events and can quantify the deposit formation rate between major shedding events. The idea is to average out the noise in the deposit mass uptake signals and to identify the larger shedding events. When the plant (and probe) artificial soot blowers are used, the probe mass signal noise level increased, and therefore, the DDF-rate determinations were not done on mass uptake signal data obtained during plant soot blower operation.

The steps involved in the deposit mass signal treatment to calculate the DDF-rate are based on Matlab procedures[30−33] as follows:

Step A: The deposit mass uptake signals are filtered using a 10 point resampling method implemented in Matlab.[30] This effectively smooths the data over 10 points, returning one resampled data point for further use.

Step B: Slope calculations are done using a moderately low order polynomial (3rd order, current case) that is

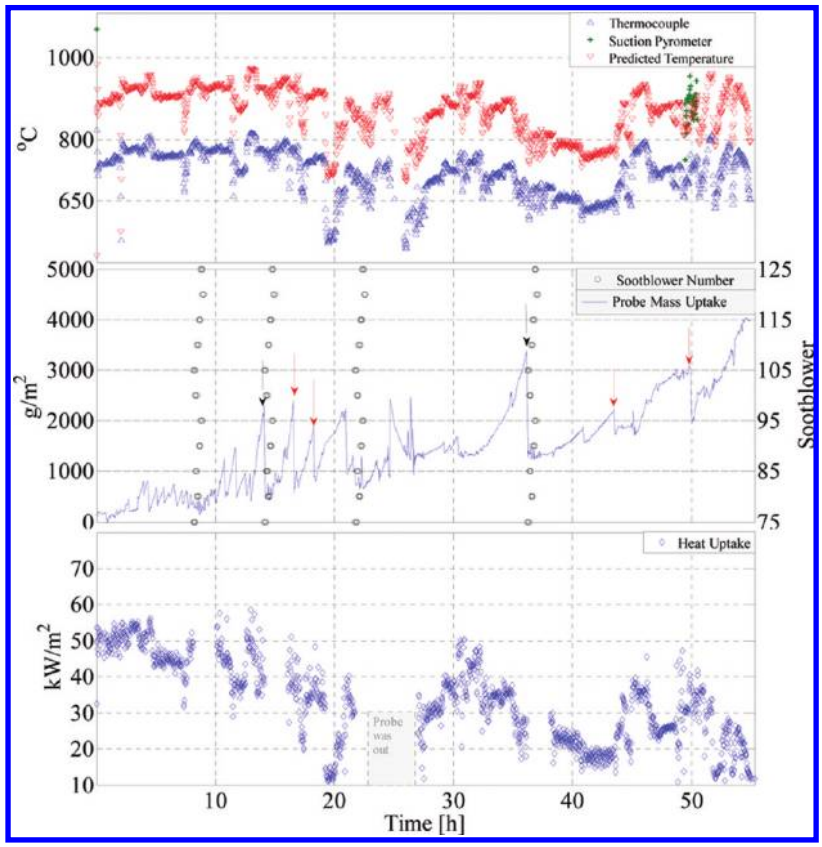

Figure 5. Raw data of flue gas temperature, deposit mass uptake, plant sootblowing events (specific number of soot blower in operation) and probe heat uptake during test 1. Red arrows with continuous line indicate natural deposit sheddings, while black arrows with discontinuous line indicate deposit shedding through plant sootblowing. The soot blower number represents a specific soot blower in the superheater region as seen on the secondary *y*-axis (middle figure).

dx.doi.org/10.1021/ef201680k | *Energy Fuels* 2012, 26, 2317−2330

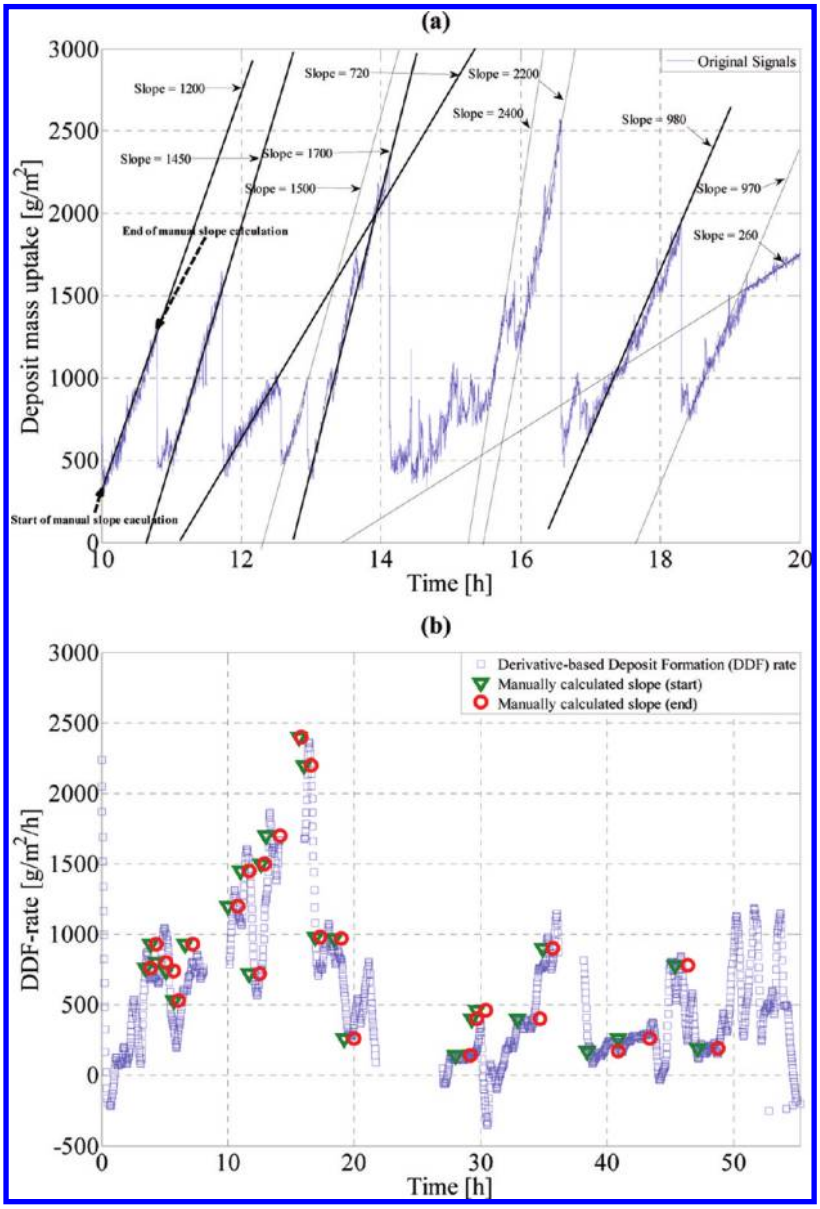

Figure 6. (a) Approximate manually calculated slopes of deposit mass uptake signals during 10−20 h of exposure time during test 1; (b) comparison of manually calculated slopes and slopes calculated by the mathematical procedure (DDF-rate) for complete test 1.

fitted to the data in a sliding window (5 data points), and finally, differentiation of the model is performed.[31]

Step C: Cut off of negative slope values is made to remove major shedding events. The cut off level is adjusted to determine the number of major shedding events accurately while still giving a satisfactory prediction of apparent deposit formation rates. A high cut off level (e.g. −200 g/(m²·h)) may count some noise as shedding events, which results in higher deposit formation rate values. A low cut off (e.g. −6000 g/(m²·h)) will include some shedding in the DDF-rate calculation and results in lower deposit formation rate values. The selected cut off level was −3800 g/(m²·h) for all the tests. This represents a subjective judgment that strikes a balance between determining the most shedding events (a high cut off level is needed) and not removing selectively a negative noise contribution to the DDF-rate determination (a low cut off level is needed).

Step D: Smoothing of the raw slope calculations is made using a moving average filter over 31 points.[32] Our choice of 15 data points on each side of the *i*th data point represents a subjective judgment that balances effective smoothing against undesired removal of minor, but significant, variations in the deposit formation rate. The result of the smoothed data is the DDF-rate.

This complete procedure was validated. It should be kept in mind that our aim is to treat all data systematically once the subjective judgments of steps C and D have been made, thus avoiding the pitfall of seeing or not seeing trends from case to case based on incomparable criteria. To validate the above described procedure of deposit formation rate determination as DDF-rates, manual slope calculations were done on the original deposit mass uptake signals of test 1. Test 1 is appropriate for comparison because the probe mass uptake signals during this test cover three kinds of behavior: (1) with small but frequent shedding events (3−10 h), (2) with large but more frequent shedding events (10−20 h), and (3) with less frequent

dx.doi.org/10.1021/ef201680k | *Energy Fuels* 2012, 26, 2317−2330

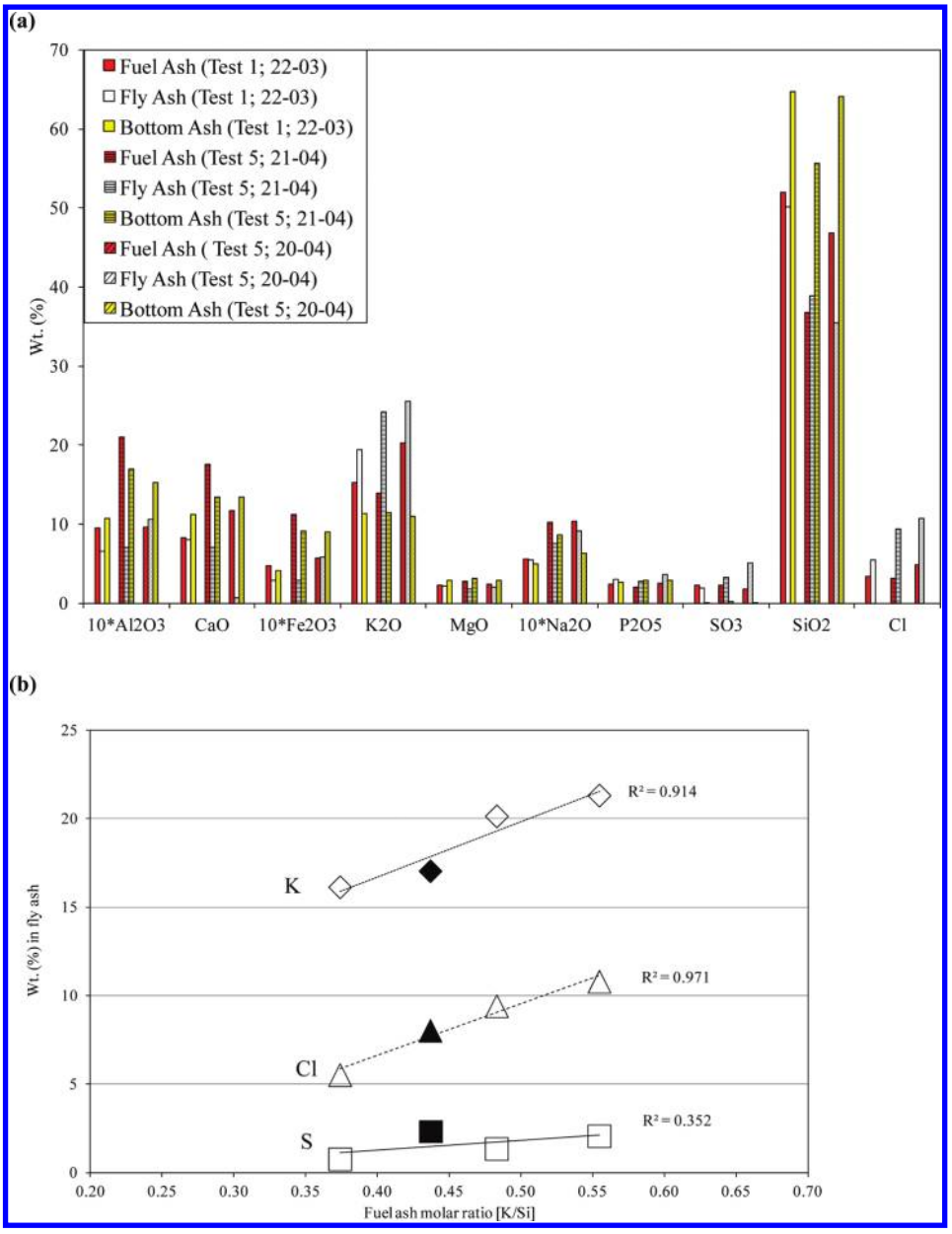

Figure 7. Ash transformation during straw and wood (straw > 46 wt %) suspension combustion: (a) comparison of fuel, fly, and bottom ash samples from tests 1 and 5; (b) impact of molar K/Si ratio in fuel ash on the content of K, Cl, and S in the fly ash. The filled points show data from straw suspension-fired measurements at Amager Unit 2,[24] while the rest of the points are from the current measurements.

shedding events (28−55 h) (Figure 5). The approximate manually calculated slopes of the 10−20 h interval during test 1 are shown in Figure 6a, and a comparison of these slopes and the calculated DDF-rates using the procedure described above is shown in Figure 6b for complete test 1. It is clear that the DDF-rates calculated by steps A through D are in good agreement with manually calculated average deposition rates. Since smoothing in step D is across shedding events, just excluding the most negative slopes in step C, the procedure results in a continuous change between the discrete levels determined by the manual procedure. This is an acceptable price to pay to get a consistent analysis of all data points and test series. The above procedure is thus adopted for the first five tests (Table 3), and the results are used to identify the influence of experimental conditions and boiler operational conditions on DDF-rates.

3.1.3. Integral Deposit Formation Rate (IDF-Rate). The deposit formation rate (g/(m²·h)) can also be determined based on the mass increase divided by a given probe exposure time, and we have called this the integral deposit formation rate (IDF-rate). The IDF-rate is then the result of both the deposit formation rate and shedding events in a given period. In this work, IDF-rates were determined using 12 h intervals. The IDF-rate is similar to deposit formation rates determined from previous full-scale measuring data.[14,24] The latter were calculated by taking the probe out, collecting the deposits, and dividing the amount of deposits by the time the probe was inside the boiler.

3.2. Chemical Compositions of Fuel Ash, Residual Ash, and Deposits. Representative samples of the fly ashes were collected from electrostatic precipitators by using a spear, while the bottom ash was collected from the water and ash pit at the bottom of the furnace. ICP-IC analysis was used to

dx.doi.org/10.1021/ef201680k | Energy Fuels 2012, 26, 2317−2330

determine the concentration of major elements in the fuel, fly, and bottom ash and deposit samples. The bulk ash compositions of the fly ashes obtained from two days (22/03/2010 and 23/03/2010) during test 1 were almost identical under almost identical operating conditions, thereby supporting the reliability of the measurements. The bulk compositions of fuel, fly, and bottom ash samples collected during test 1 and 5 are shown in Figure 7a. It is seen that the content of the most of the volatile elements (K, Cl, S) in the fly ash (colorless bars) are greater than in the fuel ash (red bars), while Ca and Si remained either almost in the same proportion or were reduced. It can also be seen that bottom ashes (yellow bars) are dominated by Si and Ca, with almost no S and Cl, possibly caused by the high volatility of S and Cl during straw and wood combustion at higher temperatures.[8,15,20,34] Compared to the fly ash from a straw grate-fired system that is rich in volatile elements, K, Cl and S, the fly ash from straw suspension firing is dominated by K, Si, and Ca.[17,19] It can also be seen that, with an increase in fuel ash K/Si molar ratio, the concentration of volatile elements, K, Cl, and, to some extent, S, increased in the fly ash (Figure 7b). This suggests that the presence of Si tends to retain K as K−silicate in the ash and residual K can bind Cl and S in the fly ash as KCl and K_2SO_4. It has also previously been reported that the fraction of water-soluble K (KCl and K_2SO_4) in the fly ash increases with increased fuel ash K/Si molar ratio.[8,34]

The composition of the probe upstream and downstream deposit layers is shown in Figure 8. The inner layers (on the upstream and on the downstream side) were rich in K, Cl, and S. K, S, and Cl were found in higher proportions on the downstream side of the probe indicating that thermophoresis and/or condensation of KCl and K_2SO_4 is important for the deposit formation process on the downstream side. The upstream side deposit outer layers contain large amounts of Si, K, and Ca, indicating that larger particles predominantly impact on and stick to the upstream side of the probe.

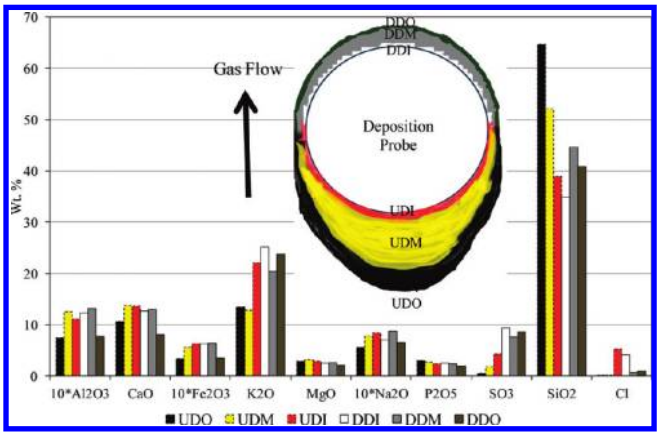

Figure 8. Bulk ash analysis of deposit layers removed from the probe after it was taken out of the boiler (straw share > 46 wt %, tests 1 and 5). UDO, upstream deposits outer layer; UDM, upstream deposits middle layer; UDI, upstream deposits innermost layer; DDI, downstream deposits innermost layer; DDM, downstream deposits middle layer; DDO, downstream deposits outer layer.

3.3. Comparison of Results with Previously Conducted Probe Measurements. Probe deposit formation measurements performed on biomass-fired boilers can be found in literature.[14,16,19,22] The ash deposit formation rates in these measurements were determined by dividing the collected amount of the probe deposit with the probe exposure time. A comparison of these previously determined probe deposit formation rates and the IDF-rates from this study (tests 1−8) is presented in Figure 9. The IDF-rate in the present study was calculated from the deposit mass uptake signals after initial 12 h to obtain data that can be compared with previous biomass suspension-fired deposit measurements.[14,24] The deposit formation rates determined in the previous full-scale measurements are also reported as IDF-rates for a better comparison.

As seen in Figure 9a, there is a general tendency that an increased alkali content in the fuel (or increased straw share in wood) and an increased flue gas temperature results in an increased IDF-rate. The trend is seen both for grate firing and suspension firing. At a flue gas temperature of 650 °C, the IDF-rate is typically from 5 to 30 g/(m^2·h) and at 900 °C, the IDF-rate is typically 20 to 110 g/(m^2·h). Skrifvars et al.[22] measured IDF-rate of 40 g/(m^2·h) at 920 °C and 7 g/(m^2·h) at 750 °C in a wood fired pulverized fuel boiler. Bashir et al.[24] measured IDF-rate of 1 g/(m^2·h) during wood suspension firing at a flue gas temperature of 586 °C, while IDF-rates of 41 g/(m^2·h) and 56 g/(m^2·h) have been measured during straw suspension firing at flue gas temperatures of about 850 °C.[14,24] Overall, the IDF-rates during straw firing in suspension and grate boilers are on similar levels, as indicated in Figure 9a. This is seen even though the percentage of fuel ash retained as fly ash can be considerably higher during suspension firing, compared to grate firing.[2]

It can be seen in Figure 9a that when firing a fuel with high alkali contents (K > 0.9 wt %, yellow and red points), the increase in IDF-rate with flue gas temperature is steeper compared to the increase in the IDF-rate with a fuel with low alkali contents (K ≤ 0.9 wt %, violet and black points). Possibly the content of gas phase alkali and the fraction of molten ash increased at increased flue gas temperatures, and both will lead to an increased deposit formation rate. It is also seen that the probe surface temperature has no significant influence on the IDF-rate (Figure 9b). The changed probe surface temperatures in the range from 400 to 650 °C do not seem to have significant influence on the deposit formation rate.

The calculated overall derivative-based deposit formation (DDF) rates were between 234 to 3105 g/(m^2·h) during tests 1−5, which are much higher than the IDF-rates. This is in agreement with expectations since IDF-rates are influenced by all shedding events during the time interval of the deposit collection. The IDF-rates provide deposit formation values that will approximately be experienced by the boiler operation personal. However, to provide more detailed information and to test models that separate the deposit formation and shedding processes, the DDF-rates data are needed.

3.4. Influence of Local Conditions on the DDF-Rate. To make it possible to investigate the influence of different operational parameters on the DDF-rates, each test was divided into further subtests based on the number of hours (usually 6 h). A significant number of data points thus allowed us to analyze the influence of local flue gas temperature and boiler operational parameters on the DDF-rates. The DDF-rate as a function of flue gas temperature is shown in Figure 10a. The figure also shows information about the applied probe temperature, straw share in wood, and deposit mass load. No significant influence of changed probe surface temperature on the DDF-rates is seen. There is observed an increase in DDF-rates with increase in flue

dx.doi.org/10.1021/ef201680k | Energy Fuels 2012, 26, 2317−2330

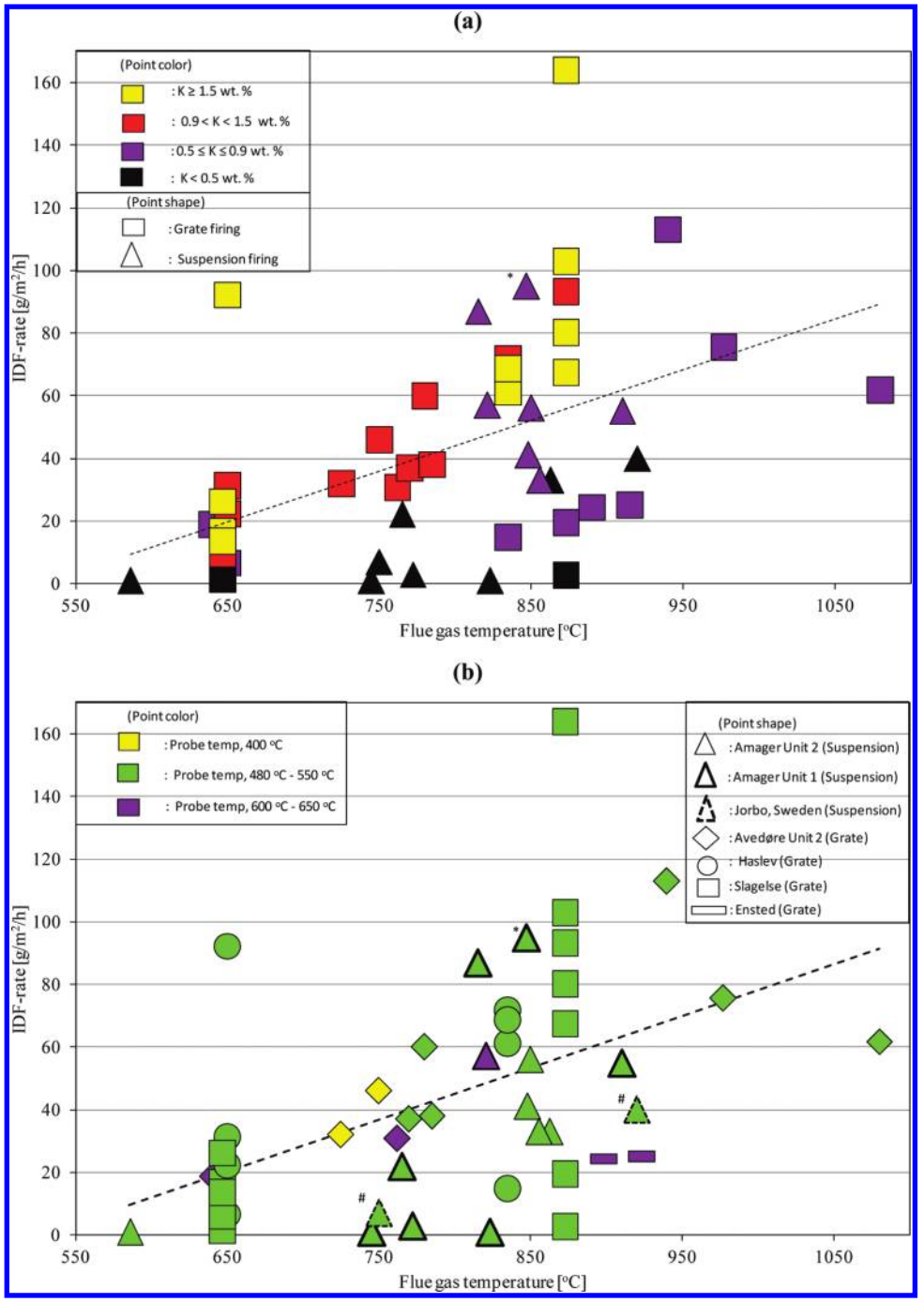

Figure 9. Impact of flue gas temperature on IDF-rates (12 h): (a) comparison of deposit probe measurements data at different fuel alkali levels and two types of straw firing technologies; (b) comparison of the some data set with marking of the probe surface temperature and boiler where the measurements were preformed. Amager Unit 2 and Unit 1 are straw and/or wood-fired suspension boilers. Jorbo, Sweden is a down-fired pulverized fuel boiler. Avedøre Unit 2, Slagelse and Ensted are straw-fired grate boilers. Haslev is a cigar type boiler where big bales of straw are fired directly.[14,16−19,22,24] Graph details: (a) the color represents the range of fuel alkali in wt %, while the particular point shape represents the straw firing technology; (b) the color represents the probe surface temperature, while the particular point shape represents the boiler type. * indicates the point where IDF-rate was calculated after 6 h. # indicates the point where the IDF-rate was measured with the short-term (about 2 h) deposit probe. For grate-fired boilers, the IDF-rate was calculated between 4 to 27 h. (Modified with permission from ref[24]. Copyright 2012, Elsevier. (Additional data of current measurements and data from Jorbo boiler were added.))

gas temperature. It can be seen that the DDF-rates increased strongly above a flue gas temperatures ranging 850−880 °C. There is only one exception and that is data from the 16/04/2010 (test 5), where a fuel particle grindability problem occurred in mill 20, and this probably caused the observed high DDF-rates. A possible reason for the increased DDF-rate at higher flue gas temperatures could be that the K−silicate and K−Ca−silicate particles hitting the probe to a higher degree are molten, and thereby a larger fraction of the impacted ash particles sticks to the deposit probe. A similar trend of increase in DDF-rate with increase in flue gas temperature was seen for the overall mean DDF-rate of each test, as shown in Figure 10b. Increased deposit

dx.doi.org/10.1021/ef201680k | Energy Fuels 2012, 26, 2317−2330

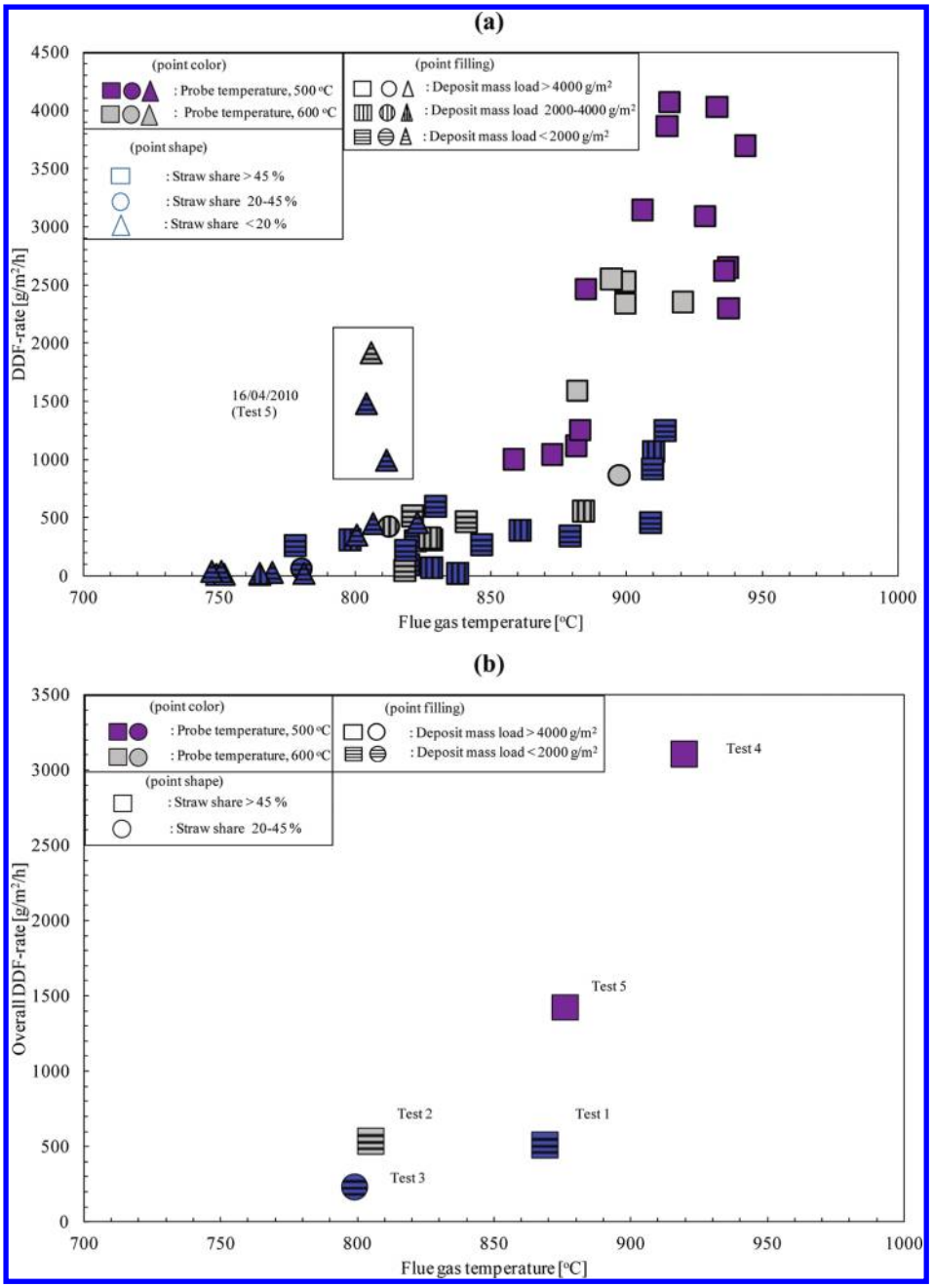

Figure 10. Impact of flue gas temperature on (a) the DDF-rate, data points from tests 1−5 and (b) overall DDF-rate, tests 1−5. Graph details: the color represents the probe surface temperature; the particular point shape represents the straw share with wood in wt %, while the particular point filling indicates the deposit mass load.

formation rate with increased flue gas temperature has also been seen in the previous full-scale measurements conducted at different straw grate-fired boilers.[14,16−19] The DDF-rate is lower at lower straw shares in wood and higher at high straw shares possibly due to the changed total fuel ash content level and changed melting properties of the fly ash. Reduced ash deposit formation rates during straw cofiring with woody biomass, compared to pure straw suspension firing have been observed by Nordgren et al.,[20] Bashir et al.,[24] and Lokare et al.[25] Lower ash deposit formation rates have been shown in previous full-scale measurements at straw grate-fired boilers for reduced alkali contents in straw.[14,16−19]

The very steep increases in the DDF-rates above approximately 850 °C are suggestive of an exponential, Arrhenius-like dependence on temperature. In Figure 11a, the logarithm of the DDF-rate is shown as function of the reciprocal of the absolute temperature. A straight line limit below which the majority of data lies is shown, but clearly a large spread is evident. The general trend is, however, followed by all points, and it appears that the data points all lie in a band between two straight lines. A similar Arrhenius-like trend is seen for overall mean DDF-rate of each test, as shown in Figure 11b. The equation of the straight line is

$$\ln(\text{DDF-rate}) = \frac{-23400}{T} + 28 \quad (5)$$

Since the full-scale measurements have been conducted in a commercial boiler, the information presented in Figures 10 and 11

dx.doi.org/10.1021/ef201680k | Energy Fuels 2012, 26, 2317−2330

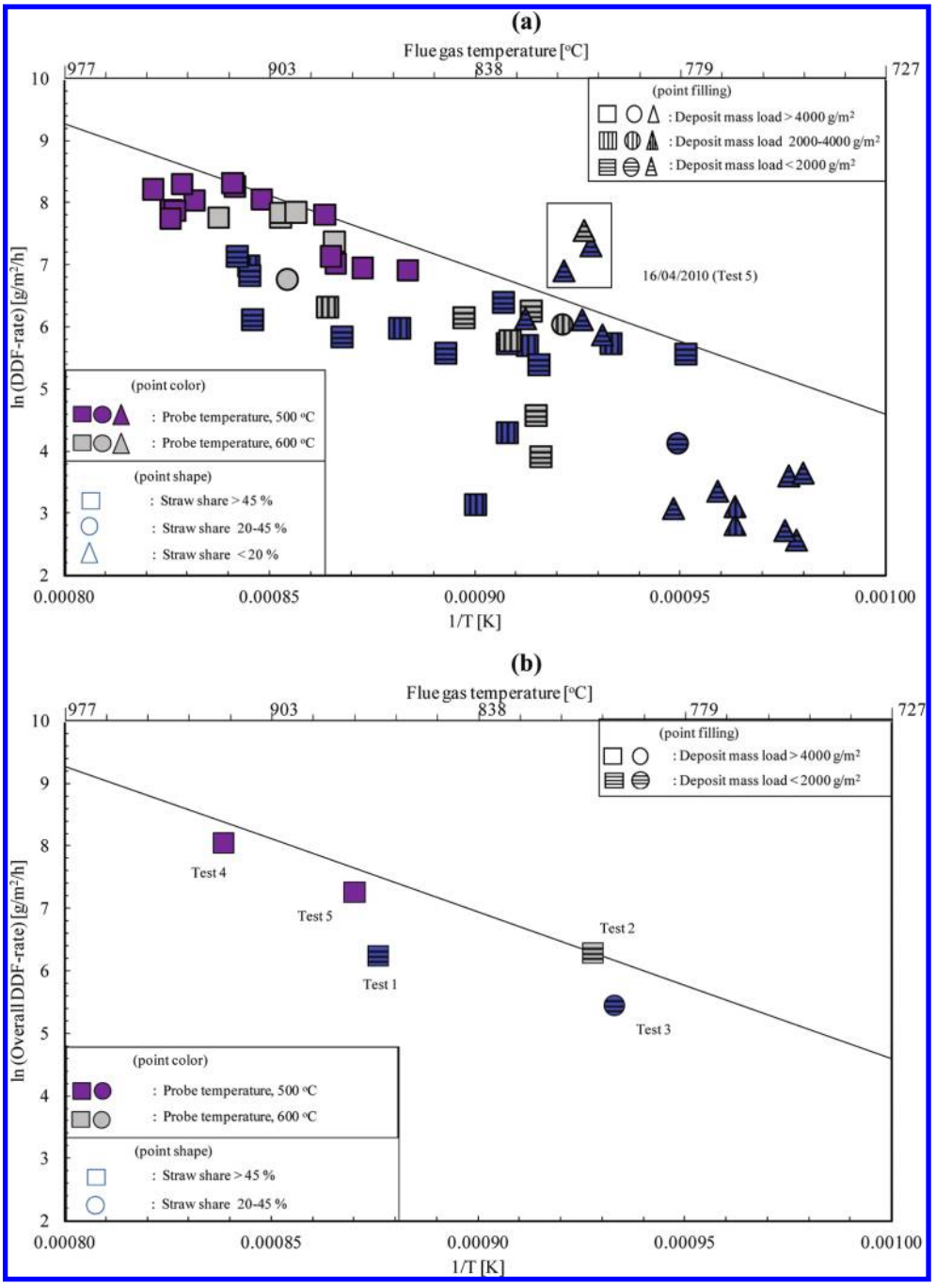

Figure 11. Logarithm of the (a) DDF-rate as a function of reciprocal of absolute flue gas temperature, data points from tests 1−5 and (b) overall DDF-rate as a function of reciprocal of absolute flue gas temperature, tests 1 to 5. Graph details: the color represents the probe surface temperature; the particular point shape represents the straw share with wood in wt %, while the particular point filling indicates the deposit mass load. The flue gas temperature in degrees Celsius is shown in the secondary *x*-axis.

may be used to predict the deposit formation rate levels in the superheater region of a biomass suspension-fired boiler. The information can be used to estimate deposit formation levels as a function of surface temperature, flue gas temperature, and fuel alkali content. Regarding the practical implications for the boiler operation personnel, the increase in probe surface temperature from 500 to 600 °C will not be a significant concern, but a higher fuel alkali contents in addition to higher fuel ash K/Si molar ratio and a flue gas temperature higher than 880 °C can result in significant deposit formation on the superheater tubes.

A prediction of fly ash melt fraction as a function of temperature based on the fly ash compositions was made by using the model proposed by Zhou et al.[35] (Figure 12). The fly ashes have a first melting temperature (FMT) between 640 and 645 °C, but at higher temperatures (>800 °C), a significant fraction of molten fly ash is seen, and this could lead to a greatly increased probability of the fly ash to stick to the deposit probe. This probably induces the higher DDF-rates at higher flue gas temperatures (Figure 10). The higher melt fraction of fly ash from test 5 may lead to a larger probability of the generated fly ash to stick to probe, causing a higher overall DDF-rate

dx.doi.org/10.1021/ef201680k | *Energy Fuels* 2012, 26, 2317−2330

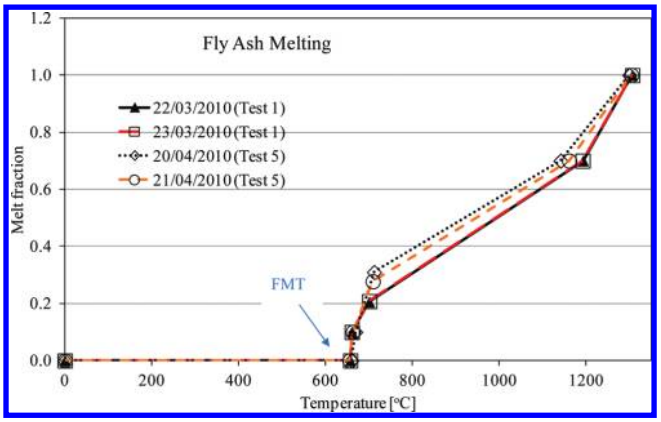

Figure 12. Fly ash melt prediction using predictive model of Zhou et al.[35]

measured for test 5 compared to test 1 (Figure 10b). The influence of fly ash composition on the melting curves indicates that the presence of the elements K, Cl, and S strongly influences the ash melt fraction.[35]

4. CONCLUSIONS

A series of full-scale probe measurements have been conducted in a biomass suspension-fired boiler to investigate ash deposit formation when firing straw and wood. The influence of fuel type, probe exposure time, probe surface temperature, and flue gas temperature on ash deposit formation rate has been investigated. A systematic procedure to determine deposit formation rate from probe measuring deposit data was developed and termed the derivative-based deposit formation rate (DDF-rate). A comparison with previously conducted probe measurements at different straw-fired boilers was made based on another measure of deposit formation rate—integral deposit formation rate (IDF-rate). Ash transformation was investigated by bulk ash analysis of the fuel ash, residual ash, and deposit layers. The overall conclusions are the following:

- The bulk chemical composition of straw and wood suspension-fired fly ash shows relatively higher contents of Si, and Ca and lower contents of volatile elements (K, Cl, and S), compared to grate firing conditions. However, it was also found that with an increase in fuel ash K/Si molar ratio the concentration of volatile elements, K, Cl, and, to some extent, S, increased in the fly ash.
- The upstream side deposit outer layers on the probe contain high concentration of Si, K, and Ca, indicating that larger particles impact on and stick to the probe on the upstream side. K, S, and Cl were found in higher proportions on the downstream side deposit layers indicating that the downstream deposits to a greater extent are formed by thermophoresis and/or condensation of KCl and K_2SO_4. The innermost layers were rich in K, Cl, and S.
- The IDF-rate increases with increased fuel K contents (straw share in wood) and with increase in flue gas temperature, but probe surface temperatures have no significant influence on the IDF-rate. The IDF-rates determined from biomass grate and suspension firing are comparable.
- The DDF-rate increases with increased straw share in wood and with increase in flue gas temperature, but probe surface temperatures have no significant influence on the measured DDF-rates.
- The overall mean DDF-rate also increases with increase in flue gas temperature and deposit formation levels between 234 to 3105 g/(m^2·h) were observed.

AUTHOR INFORMATION

Corresponding Author

*Phone: +45 45252849. Fax: +45 45882258. E-mail: paj@kt.dtu.dk.

Notes

The authors declare no competing financial interest.

ACKNOWLEDGMENTS

The financial support by Energinet.DK under the PSO project 7217 and the financial support by Vattenfall A/S are gratefully acknowledged. Special thanks to Vattenfall A/S for providing access to their boiler. In addition, we are thankful to the operational staff at the Amager Power Plant for their technical support during the power plant boiler measurements.

NOMENCLATURE

A, B, C, D, E, F = empirical constants for flue gas temperature prediction
CCD = charge-coupled device
DDF-rate = derivative-based deposit formation rate (g/(m^2·h))
$Diff_{pred}$ = predicted difference between thermocouple based flue gas temperature measurements and suction pyrometer based flue gas temperature measurements (°C)
FMT = first melting temperature (°C)
ICP-IC = inductively coupled plasma-ion chromatography
IDF-rate = integral deposit formation rate (g/(m^2·h))
IFRF = International Flame Research Foundation
g = gravitational acceleration (m/s^2)
L_1 = distance from the hinge to the balance (m)
L_2 = distance from the hinge to the mass center of the deposit (m)
m_d = deposit mass (g)
m_{t0} = initial signal of the load cell (g)
m_{t1} = final signal of the load cell (g)
T = flue gas temperature (K)
X_i = operational parameter for flue gas temperature prediction
Y_{calc} = predicted flue gas temperature (°C)
Y_{meas} = measured suction pyrometer flue gas temperature (°C)
Y_{TC} = measured thermocouple flue gas temperature (°C)

REFERENCES

(1) Montgomery, M.; Jensen, S. A.; Borg, U.; Biede, O.; Vilhelmsen, T. Experiences with high temperature corrosion at straw-firing power plants in Denmark. *Mater. Corros.* **2011**, *62*, 593−605.
(2) Nielsen, H. P. Deposition and high temperature corrosion in biomass-fired boilers. PhD Thesis, Technical University of Denmark. 1998; ISBN 87-90142-47-0.
(3) Jenkins, B. M.; Baxter, L. L.; Miles, T. R. Jr.; Miles, T. R. Combustion properties of biomass. *Fuel Process. Technol.* **1998**, *54*, 17−46.
(4) Munir, S.; Nimmo, W.; Gibbs, B. M. Co-combustion of agricultural residues with coal: turning waste into energy. *Energy Fuels* **2010**, *24*, 2146−2153.
(5) Shao, Y.; Xu, C.; Zhu, J.; Preto, F.; Wang, J.; Tourigny, G.; Badour, C.; Li, H. Ash deposition during cofiring biomass and coal in a fluidized-bed combustor. *Energy Fuels* **2010**, *24*, 4681−4688.
(6) Sander, B.; Henriksen, N.; Larsen, O. H.; Skriver, A.; Ramsgaard-Nielsen, C.; Jensen, J. N.; Stærkind, K.; Livberg, H.; Thellefsen, M.;

Dam-Johansen, K.; Frandsen, F. J.; van der Lans, R.; Hansen, J. Emissions, corrosion, and alkali chemistry in straw-fired combined heat and power plants. *Proceedings of 1st World Conference on Biomass for Energy and Industry*, Sevilla, June 5−9, 2009.
(7) Jensen, P. A.; Sander, B.; Dam-Johansen, K. Removal of K and Cl by leaching of straw char. *Biomass Bioenergy* **2001**, *20*, 447−457.
(8) Frandsen, F. J. Ash formation, deposition, and corrosion when utilizing straw for heat and power production. Doctoral Thesis, Technical University of Denmark. 2011; ISBN 978-87-92481-40-5.
(9) Baxter, L. L. Ash deposition during biomass and coal combustion: A mechanistic approach. *Biomass Bioenergy* **1993**, *4*, 85−102.
(10) Andersen, K. H.; Frandsen, F. J.; Hansen, P. F. B.; Wieck-Hansen, K.; Rasmussen, I.; Overgaard, P.; Dam-Johansen, K. Deposit formation in a 150 MWe utility PF-boiler during co-combustion of coal and straw. *Energy Fuels* **2000**, *14*, 765−780.
(11) Jensen, P. A.; Frandsen, F. J.; Hansen, J.; Dam-Johansen, K.; Henriksen, N.; Hörlyck, S. SEM investigation of superheater deposits from biomass-fired boilers. *Energy Fuels* **2004**, *18*, 378−384.
(12) Zbogar, A.; Frandsen, F.; Jensen, P. A.; Glarborg, P. Shedding of ash deposits. *Prog. Energy Combust. Sci.* **2009**, *35*, 31−56.
(13) Jensen, P. A.; Zhou, H.; Frandsen, F. J.; Hansen, J. Ash deposits removal in biomass power plant boilers. *Proceeding of 15th European Biomass Conference and Exhibition*, Berlin, Germany, May 7−11, 2007.
(14) Tobiasen, L.; Skytte, R.; Pedersen, L. S.; Pedersen, S. T.; Lindberg, M. A. Deposit characteristics after injection of additives to a Danish straw-fired suspension boiler. *Fuel Process. Technol.* **2007**, *88*, 1108−1117.
(15) Wu, H.; Glarborg, P.; Frandsen, F. J.; Dam-Johansen, K.; Jensen, P. A. Dust-firing of straw and additives: Ash chemistry and deposition behavior. *Energy Fuels* **2011**, *25*, 2862−2873.
(16) Jensen, P. A.; Stenholm, M.; Hald, P. Deposition investigation in straw-fired boilers. *Energy Fuels* **1997**, *11*, 1048−1055.
(17) Zhou, H.; Frandsen, F. J.; Jensen, P. A.; Glarborg, P. *PSO Project 4106, CHEC Report R0603*; CHEC Research Centre, Technical University of Denmark: Kongens Lyngby, Denmark, 2006.
(18) Zbogar, A.; Frandsen, F. J.; Jensen, P. A.; Hansen, J.; Glarborg, P. Experimental investigation of ash deposit shedding in a straw-fired boiler. *Energy Fuels* **2006**, *20*, 512−519.
(19) Hansen, J.; Jensen, P. A.; Glarborg, P. *Deposit Probe Measurements in the Avedøre and Ensted Straw-Fired Grate Boilers*, CHEC Report R0705, CHEC Research Centre, Technical University of Denmark: Kongens Lyngby, Denmark, 2007.
(20) Nordgren, D.; Hedman, H.; Padban, N.; Boström, D.; Öhman, M. Ash transformations in pulverised fuel co-combustion of straw and woody biomass. *Fuel Process. Technol.* **2011**, DOI: 10.1016/j.fuproc.2011.05.027.
(21) Theis, M.; Skrifvars, B. J.; Hupa, M.; Tran, H. Fouling tendency of ash resulting from burning mixtures of biofuels. Part 1: Deposition rates. *Fuel* **2006**, *85*, 1125−1130.
(22) Skrifvars, B.-J.; Lauren, T.; Hupa, M.; Korbee, R.; Ljung, P. Ash behavior in a pulverized wood fired boiler—A case study. *Fuel* **2004**, *83*, 1371−1379.
(23) *IFRF Handbook*, ISSN: 1607-9116. Available online: www.handbook.ifrf.net/handbook/index.html (accessed: Jan. 30, 2009).
(24) Bashir, M. S.; Jensen, P. A.; Frandsen, F.; Wedel, S.; Dam-Johansen, K.; Wadenbäck, J.; Pedersen, S. T. Ash transformation and deposit build-up during biomass suspension and grate firing: Full-scale experimental studies. *Fuel Process. Technol.* **2012**, *97*, 93−106.
(25) Lokare, S. S.; Dunaway, J. D.; Moulten, D.; Rogers, D.; Tree, D. R.; Baxter, L. L. Investigation of ash deposition rates for a suite of biomass fuels and fuel blends. *Energy Fuels* **2006**, *20*, 1008−1014.
(26) Gjernes, E. Fuel flexibility at Amager unit 1 using pulverized fuels. *Proceedings of Power-Gen Europe*, Cologne, Germany, 2006.
(27) *IFRF Suction Pyrometer, User Information Document*; International Flame Research Foundation: 2007.
(28) Kittrel, J. R. *Adv. Chem. Eng.* **1970**, *8*, 97−183.
(29) Pritchard, D. J.; Bacon, D. W. Prospects for reducing correlation among parameters estimates in kinetics models. *Chem. Eng. Sci.* **1978**, *33*, 1539−1543.
(30) *Matlab, Signal Processing Toolbox*. http://www.mathworks.com/help/toolbox/signal/resample.html (Accessed: March 31, 2011).
(31)http://www.mathworks.com/matlabcentral/fileexchange/16997-movingslope (Accessed: Dec. 16, 2010).
(32) Smith, S. W. *The Scientist and Engineer's Guide to Digital Signal Processing*; Calfornial Technical Publishing: San Diego, CA, 1997−1998; Chapter 15, pp 277−284. Available online: http://www.dspguide.com/ (Accessed: Dec. 31, 2010).
(33) *Matlab, Curve Fitting Toolbox*. http://www.mathworks.com/help/toolbox/curvefit/bq_6yqb.html (Accessed: March 31, 2011).
(34) Zheng, Y.; Jensen, P. A.; Jensen, A. D.; Sander, B.; Junker, H. Ash transformation during co-firing coal and straw. *Fuel* **2007**, *86*, 1008−1020.
(35) Zhou, H.; Jensen, P. A.; Frandsen, F. J. Dynamic mechanistic model of superheater deposit growth and shedding in a biomass fired grate boiler. *Fuel* **2007**, *86*, 1519−1533.